PROCEEDINGS OF SCIENCE

PoS(QCHSC24)218

Nonequilibrium Dynamics of High Density Matter under a Strong Magnetic Field

Gastão Krein*

Instituto de Física Teórica, Universidade Estadual Paulista
Rua Dr. Bento Teobaldo Ferraz, 271 - Bloco II, 01140-070 São Paulo, SP, Brasil

E-mail: gastao.krein@unesp.br

I present recent results on the nonequilibrium dynamics of strongly interacting matter in the presence of strong magnetic fields. First, I discuss the influence of a strong magnetic field on the time evolution of the quark condensate (scalar density) at finite temperature, studied within the linear sigma model. The dynamics of the condensate are governed by a Ginzburg–Landau–Langevin equation derived using the closed-time path (CTP) formalism of nonequilibrium quantum field theory. I then introduce a relativistic field-theoretical framework to model quark substructure effects in nucleons through deformed anticommutation relations. Preliminary results in the mean-field approximation reveal how these modifications affect the equilibrium properties of dense matter. This combined approach provides a promising framework for future investigations of magnetic field effects in both hot and cold baryonic systems.

The XVIth Quark Confinement and the Hadron Spectrum Conference (QCHSC24)
19-24 August, 2024
Cairns Convention Centre, Cairns, Queensland, Australia

*Speaker

https://pos.sissa.it/

1. Introduction

Strong magnetic fields, like high temperatures and large baryon densities, influence the properties of quantum chromodynamics (QCD) in various physical contexts, such as the early universe, compact stars, and heavy-ion collisions [1]. All of these environments involve time evolution. In this communication, I present recent results from studies addressing the time evolution of a key QCD property: the chiral quark condensate. The chiral condensate serves as an order parameter for spontaneous chiral symmetry breaking. Chiral symmetry is an approximate symmetry of the QCD Lagrangian in the light-quark sector, spontaneously broken in the vacuum and potentially restored at high temperature and baryon density. It acquires particular significance in the QCD phase diagram, particularly in the temperature T versus baryon density ρ (or baryon chemical potential μ_B) plane. In ordinary nuclear matter—composed of protons and neutrons bound in atomic nuclei and characterized[1] by $T \approx 0$ and $\rho \sim 0.15$ fm^{-3}—the quark condensate is nonzero, signaling a symmetry-broken phase. At high temperatures (typically $T > 100$ MeV) and $\rho \sim 0$, the system enters the quark-gluon plasma phase, where the condensate is small and chiral symmetry is approximately restored. Low T and high ρ characterize dense QCD matter, such as that found in compact objects like neutron stars, where the condensate is also small and indicates approximate chiral symmetry.

The influence of strong magnetic fields on the QCD phase diagram has been extensively studied using first-principles QCD methods in two limiting regimes: at high temperatures and zero baryon density, primarily through lattice QCD [2]; and at high baryon densities and zero temperature, via perturbative QCD [3]. In contrast, no first-principles QCD methods exist to tackle magnetic field effects in the intermediate regime—characterized by low temperatures and baryon densities ranging from one to about five times the nuclear saturation density, $\rho_{\text{sat}} \approx 0.15$ fm^{-3}. This region of the phase diagram is particularly challenging to describe because as ρ increases, nucleons may begin to spatially overlap while not yet fully dissolving into deconfined quarks and gluons, leading to strong many-body and medium effects. The complex interplay among confinement, chiral symmetry, and many-body correlations in this regime makes it one of the most intriguing and difficult frontiers in the study of QCD matter.

To address this challenging regime of overlapping nucleons, I begin by presenting selected results on the influence of magnetic fields on the time evolution of the chiral condensate in quark matter [4]. These results were obtained within the linear sigma model with quarks, where the temporal evolution of the condensate is described by a Ginzburg–Landau–Langevin (GLL) equation. The GLL equation was derived from a two-particle irreducible (2PI) effective action computed using the closed-time path (CTP) formalism of nonequilibrium quantum field theory. I will then discuss a field-theoretic approach to study the nuclear many-body problem with composite nucleons, designed to be combined with the CTP formalism to study magnetic field effects in cold and dense nuclear matter.

[1] We use $\hbar = c = k_B = 1$ throughout this communication.

2. Quark matter

The physical scenario of interest involves a rapid phase transition at a given instant from a thermodynamic equilibrium phase to a nonequilibrium phase. The goal is to describe how the nonequilibrium state evolves over time. Here, the system under consideration is quark matter in the presence of an external magnetic field, with thermodynamic phases distinguished by the value of the chiral quark condensate. The phase change of interest is from a chirally restored to a chirally broken phase. In this work, the time evolution of the condensate is described by a Ginzburg-Landau-Langevin (GLL) field equation. GLL equations are widely employed in field-theoretic studies of dynamical phase transitions [5, 6]. In condensed matter physics, a prototypical example of such a transition is a temperature quench in a spin system, where a sudden drop in temperature drives the system irreversibly from a spin-disordered to a spin-ordered phase; the order parameter in this situation is the magnetization of the system. The GLL equations in that context are typically either phenomenological or derived from a microscopic model via coarse-graining procedures—Ref. [4] provides an extensive list of references on these approaches.

The GLL equation for the quark condensate dynamics was derived in Ref. [4] from the linear sigma model [7] with quarks (LSMq), coupled to an external magnetic field. For completeness and to set notation, we present the Lagrangian:

$$\mathcal{L} = \bar{q}[i\partial\!\!\!/ - g(\sigma + i\gamma_5 \boldsymbol{\tau}\cdot\boldsymbol{\pi})]q + \frac{1}{2}\left[\partial_\mu\sigma\partial^\mu\sigma + \partial_\mu\boldsymbol{\pi}\cdot\partial^\mu\boldsymbol{\pi}\right] - \frac{\lambda}{4}(\sigma^2 + \boldsymbol{\pi}^2 - v^2)^2 - h_q\sigma - U_0, \quad (1)$$

where $q = (u, d)^T$ is the light-quark isodoublet, while σ and $\boldsymbol{\pi}$ denote scalar-isoscalar and pseudoscalar-isotriplet fields, respectively, coupled to quarks via Yukawa coupling g. The constant U_0 sets the classical vacuum energy to zero. The metric is $g^{\mu\nu} = (1, -1, -1, -1)$ and the conventions for the Dirac matrices are those of Bjorken–Drell [8]. Model parameters can be tuned to reproduce chiral observables. At tree level, for instance, $h_q = f_\pi m_\pi^2$, $v^2 = f_\pi^2 - m_\pi^2/\lambda$, $m_\sigma^2 = 2\lambda f_\pi^2 + m_\pi^2$, and $m_q = g\langle\sigma\rangle$, where f_π and m_π are the pion decay constant and mass, m_σ the sigma meson mass, and m_q the constituent quark mass. The external magnetic field enters via minimal substitution: $\partial_\mu \to D_\mu = \partial_\mu + iqA_\mu$, with A_μ the electromagnetic field and q the quark charge. In Ref. [4], pions were neglected and so dissipation arises solely from $\sigma \leftrightarrow \bar{q}q$ processes.

The derivation of the GLL equation in Ref. [4] extends the semiclassical framework from Ref. [9] to include the effects of an external magnetic field. This approach relies on the Schwinger-Keldysh closed-time path (CTP) formalism [10, 11] and the Feynman-Vernon influence functional [12], as applied in nonequilibrium quantum field theory [13, 14]. The effective semiclassical action is

$$\Gamma[\sigma, S] = \Gamma_{\rm cl}[\sigma] + i\,{\rm Tr}\ln S - i\,{\rm Tr}\left(iD\!\!\!\!/ - m_0\right)S + \Gamma_2[\sigma, S]\,, \quad (2)$$

with $\Gamma_2[\sigma, S]$ given by:

$$\Gamma_2[\sigma, S] = g\int_C d^4x\, {\rm tr}\left[S^{++}(x,x)\sigma^+(x) + S^{--}(x,x)\sigma^-(x)\right]\,, \quad (3)$$

where tr means trace over color, flavor, and Dirac indices, the scalar fields $\sigma^\pm$ and the quark propagators S_{++}, S_{--}, and $S_\pm$ are defined on the Schwinger-Keldysh contour C shown in Fig. 1. The two fields $\sigma^\pm(x)$ are not independent; they couple through the CTP boundary condition

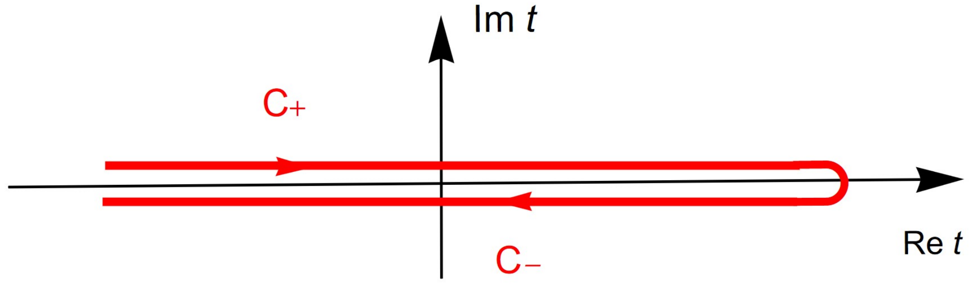

Figure 1: Schwinger-Keldish contour.

$\sigma^+(T, \boldsymbol{x}) = \sigma^-(T, \boldsymbol{x})$ where $T \to +\infty$ (borders of the CTP contour) so that there is a single mean field $\sigma(x)$ given by the equation of motion motion [13]:

$$\left.\frac{\delta\Gamma[\sigma, S]}{\delta\sigma^\pm(x)}\right|_{\sigma^+=\sigma^-=\sigma} = 0 \,. \tag{4}$$

Quarks are integrated out via their equation of motion:

$$\frac{\delta\Gamma[\sigma, S]}{\delta S^{ab}(x, y)} = 0 \,, \tag{5}$$

yielding

$$\big(i\not{D} - g\sigma_0(x)\big)\, S^{ab}(x, y) - \int_C d^4z\, \frac{\delta\Gamma_2}{\delta S^{ac}(x, z)}\, S^{cb}(z, y) = i\delta^{ab}\delta^{(4)}(x - y). \tag{6}$$

Solving these equations exactly is impractical. A feasible approximation [4, 9] involves expanding around local equilibrium, akin to hydrodynamic descriptions:

$$\sigma^a(x) = \sigma_0^a(x) + \delta\sigma^a(x) \,, \tag{7}$$

$$S^{ab}(x, y) = S^{ab}_{\rm thm}(x, y) + \delta S^{ab}(x, y) + \delta^2 S^{ab}(x, y) + \cdots \,. \tag{8}$$

The equilibrium components σ_0 and $S^{ab}_{\rm thm}$ satisfy

$$\frac{\delta\Gamma_{\rm cl}}{\delta\sigma_0^a(x)} = -g{\rm Tr}S^{aa}(x, x) \,, \tag{9}$$

$$\big[i\not{D} - m_0 - g\,\sigma_0(x)\big]\, S^{ab}_{\rm thm}(x, y) = -i\delta^{ab}\delta^{(4)}(x - y). \tag{10}$$

Solutions can be obtained iteratively [4, 9]. For a uniform magnetic field, Ref. [4] solves Eq. (10) using the lowest Landau level (LLL) approximation (valid for strong magnetic fields). In momentum space, assuming $\boldsymbol{B} \parallel \hat{z}$ and defining $\boldsymbol{p}_\perp^2 = p_x^2 + p_y^2$, $p_\parallel^2 = p_0^2 - p_z^2$, the thermal quark propagators read:

$$S^{++}_{\rm thm}(p) = e^{-\boldsymbol{p}_\perp^2/|q_f B|}\, A(p) \left[\frac{i}{p_\parallel^2 - m_q^2 + i\epsilon} - 2\pi n_F(p_0)\delta(p_\parallel^2 - m_q^2) \right], \tag{11}$$

$$S^{+-}_{\rm thm}(p) = e^{-\boldsymbol{p}_\perp^2/|q_f B|}\, A(p)\, 2\pi\delta(p_\parallel^2 - m_q^2)\, [\theta(-p_0) - n_F(p_0)]\,, \tag{12}$$

$$S^{-+}_{\rm thm}(p) = e^{-\boldsymbol{p}_\perp^2/|q_f B|}\, A(p)\, 2\pi\delta(p_\parallel^2 - m_q^2)\, [\theta(p_0) - n_F(p_0)]\,, \tag{13}$$

$$S^{--}_{\rm thm}(p) = e^{-\boldsymbol{p}_\perp^2/|q_f B|}\, A(p) \left[\frac{-i}{p_\parallel^2 - m_q^2 - i\epsilon} - 2\pi n_F(p_0)\delta(p_\parallel^2 - m_q^2) \right], \tag{14}$$

where $A(p) = (\not{p}_\parallel + m_q)[1 + i\gamma^1\gamma^2 \text{sign}(qB)]$, $\not{p}_\parallel = \gamma^0 p_0 - \gamma^3 p_z$, $m_q = g\sigma_0$, and n_F is the Fermi-Dirac distribution:

$$n_F(p_0) = \frac{1}{e^{|p_0|/T} + 1}. \tag{15}$$

The anisotropy between $\boldsymbol{p}_\perp$ and p_z in these propagators lead to anisotropic dynamics for the condensate. Since the action $\Gamma[\sigma, S]$ is complex, variation w.r.t. $\sigma^\pm$ to obtain an e.o.m. is not a well-defined operation. The Feynman-Vernon trick is used to obtain a real-valued action by integrating out the imaginary part in favor of a noise field. This leads to a Langevin equation for σ that contains memory. To deal with memory effects, the *linear harmonic approximation*, in that the memory dynamics are effectively taken into account by soft-mode (long wavelengths) harmonic oscillations around a mean field—for details, see Refs. [4, 9]. These steps lead to the following GLL equation in coordinate space [4]:

$$\frac{\partial^2 \sigma(t,\boldsymbol{x})}{\partial t^2} - \nabla^2\sigma(t,\boldsymbol{x}) + \eta\frac{\partial\sigma(t,\boldsymbol{x})}{\partial t} + F_\sigma = \xi(t,\boldsymbol{x})\ , \tag{16}$$

where $\boldsymbol{x}$ stands for $\boldsymbol{x}_\perp = (x, y)$, F_σ is the free energy

$$F_\sigma = \lambda\sigma\left(\sigma^2 - f_\pi^2 + \frac{m_\pi^2}{\lambda}\right) - f_\pi m_\pi^2 + g\rho_s^B(\sigma_0) + g\rho_s^{BT}(\sigma_0)\ , \tag{17}$$

and $\rho_s^B(\sigma_0)$ and $\rho_s^{TB}(\sigma_0)$ are contributions to the scalar density $\rho_s(\sigma_0)$:

$$\rho_s^B(\sigma_0) = -\frac{N_c}{2\pi^2}\, m_q \sum_{f=u,d} |q_f B| \left[\ln\Gamma(x_f) - \frac{1}{2}\ln 2\pi + x_f - \frac{1}{2}(2x_f - 1)\ln x_f\right]\ , \tag{18}$$

$$\rho_s^{BT}(\sigma_0) = -\frac{N_c}{\pi^2} m_q\big(|q_u B| + |q_d B|\big) \int_0^\infty dp_z \frac{n_F(E_q(p_z))}{E_q(p_z)} \tag{19}$$

η is the dissipation coefficient:

$$\eta = g^2\frac{N_c}{4\pi}\,[1 - 2n_F(m_\sigma/2)]\,\frac{1}{m_\sigma^2}(eB)\sqrt{m_\sigma^2 - 4m_q^2}\ . \tag{20}$$

In the above, $N_c = 3$ is the number of colors, q_f is equal to $2/3\,e$ for the u quark and -$1/3\,e$ for the d quark, $x_f = m_q^2/2|q_f B|$, and Γ is the Euler gamma function. Note that flavor symmetry is being used: $m_u = m_d = m_q = g\sigma_0$. The quantity η also controls the fluctuations as it enters in the noise correlation function:

$$\langle \xi(t,\boldsymbol{x})\, \xi(t',\boldsymbol{x}') \rangle = \eta\, m_\sigma \coth(m_\sigma/2T)\, \delta(t-t')\, \frac{1}{L}\, \delta(\boldsymbol{x}-\boldsymbol{x}'). \tag{21}$$

These quantities depend on m_σ and m_q which, in turn, depend on T and eB, implying they are not put in by hand, but calculated. The factor $1/L$ comes from the fact that the field dynamics of σ occur in the (x, y) plane (but the mass dimension of σ is still equal to unity).

In summary, Eq. (16) governs the nonequilibrium dynamics of the quark condensate, incorporating both dissipation and noise. These effects are driven by the damping coefficient η_σ, which itself arises from $\sigma \leftrightarrow \bar{q}q$ processes: η_σ vanishes when the σ meson energy satisfies $E_\sigma < 2m_q$. The equilibrium values of both the quark and σ masses are modified by the presence of a magnetic field. Consequently, the temperature dependence of η_σ for $B \neq 0$ differs from that in the $B = 0$ case [4]. When pions are included, dissipation is expected to increase further due to additional $\sigma \leftrightarrow \pi\pi$ processes.

Next, I present representative numerical solutions of Eq. (16) within a quench scenario. The couplings g and λ are chosen to produce a crossover transition at $T_{\rm pc} \simeq 150$ MeV for $B = 0$, with $g = 3.3$ and $\lambda = 20$. These values yield vacuum masses $m_\sigma = 604$ MeV and $m_q = 290$ MeV. Figure 2 displays the time evolution of the spatial average of $\sigma(\boldsymbol{x}_\perp, t)$:

$$\overline{\sigma}(t) = \frac{1}{L^2} \int_{L^2} d\boldsymbol{x}_\perp\, \sigma(\boldsymbol{x}_\perp, t). \tag{22}$$

The results correspond to a single realization of the noise, with $eB = 20\, m_\pi^2$, and two different temperature quenches: $T_{\rm qch} = 50$ MeV and $T_{\rm qch} = 100$ MeV, for which $\eta = 2.55$ fm^{-1} and $\eta = 2.23$ fm^{-1}, respectively [15].

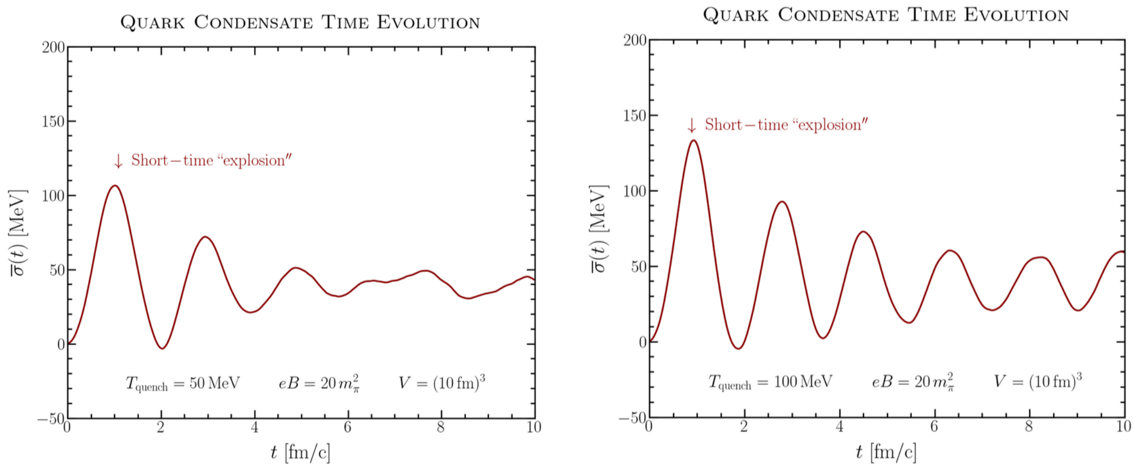

Figure 2: Time dependence of spatial average of the quark condensate [15].

As seen in Fig. 2, two key features of a quenched dynamical phase transition are clearly visible: a rapid initial rise—referred to as the "short-time explosion"—followed by long-time damped oscillations. The initial rapid growth takes approximately 1 fm/c after the quench in both cases. For the lower quench temperature ($T_{\rm qch} = 50$ MeV), the field appears to thermalize within about

10 fm/c. However, for the higher quench temperature ($T_{\rm qch} = 100$ MeV), thermalization is not achieved within this timescale. For reference, the typical lifetime of the quark-gluon plasma in a heavy-ion collision before hadronization is also of the order of 10 fm/c.

3. Nuclear matter - nucleon superposition

At sufficiently high baryon densities, the quark wave functions of different nucleons begin to overlap and become delocalized, potentially leading to a percolation-like phenomenon [16, 17]. The average distance between two nucleons in nuclear matter at baryon density ρ is given by $d_{NN} \sim \rho^{-1/3}$. For normal nuclear matter density $\rho_{\rm sat}$, this distance is $d^{\rho_{\rm sat}}_{NN} = 1.88$ fm; at $\rho = 5\rho_{\rm sat}$, it decreases to $d^{5\rho_{\rm sat}}_{NN} \sim d^{\rho_{\rm sat}}_{NN}/2$. From a purely geometrical perspective, taking the nucleon as a spherical bag with radius $R_N \sim 0.8$ fm—a typical value in the cloudy bag model [18]—it becomes evident that quark wave functions from different nucleons can significantly overlap at high densities. However, this geometrical viewpoint is overly simplistic; in reality, quark delocalization may be far more complex due to quantum fluctuations, which could give rise to a much richer and more intricate quark delocalization landscape.

Modeling such a system is challenging because nucleons cease to be appropriate degrees of freedom once they begin to lose their individual identities in high-density nuclear matter. This complexity can be illustrated using a nonrelativistic framework. Consider a three-quark nucleon state defined as $|N\rangle = \hat{B}^\dagger_N|0\rangle$, with $N = \{\boldsymbol{P}, m_S, m_I\}$ denoting the nucleon's center-of-mass momentum, spin, and isospin projections. Here, $|0\rangle$ is the vacuum state satisfying $\hat{B}_N|0\rangle = 0$.

The nucleon creation operator can be expressed in terms of quark creation operators as (with repeated indices summed over) [19–21]:

$$\hat{B}^\dagger_N = \frac{1}{\sqrt{3!}}\,\Psi^{\mu_1\mu_2\mu_3}_N\,\hat{q}^\dagger_{\mu_1}\hat{q}^\dagger_{\mu_2}\hat{q}^\dagger_{\mu_3}, \quad \text{with} \quad \Psi^{\mu_1\mu_2\mu_3 *}_{N'}\Psi^{\mu_1\mu_2\mu_3}_N = \delta_{N'N}, \tag{23}$$

where μ collectively labels spatial (momentum) and internal (spin, color, flavor) quantum numbers. The quark creation and annihilation operators satisfy the canonical anticommutation relations:

$$\{\hat{q}_\mu, \hat{q}^\dagger_\nu\} = \delta_{\mu\nu}, \quad \{\hat{q}_\mu, \hat{q}_\nu\} = \{\hat{q}^\dagger_\mu, \hat{q}^\dagger_\nu\} = 0. \tag{24}$$

Using these, one finds [19–21]

$$\langle N'|N\rangle = \langle 0|\hat{B}_{N'}\hat{B}^\dagger_N|0\rangle = \Psi^{\mu_1\mu_2\mu_3 *}_{N'}\Psi^{\mu_1\mu_2\mu_3}_N = \delta_{N'N}, \tag{25}$$

$$\{\hat{B}_{N'}, \hat{B}^\dagger_N\} = \delta_{N'N} - \hat{\Delta}_{N'N}, \quad \{\hat{B}_{N'}, \hat{B}_N\} = 0, \tag{26}$$

$$\hat{\Delta}_{N'N} = 3\Psi^{*\mu_1\mu_2\mu_3}_{N'}\Psi^{\mu_1\mu_2\nu_3}_N\,\hat{q}^\dagger_{\nu_3}\hat{q}_{\mu_3} - \frac{3}{2}\Psi^{*\mu_1\mu_2\mu_3}_{N'}\Psi^{\mu_1\nu_2\nu_3}_N\,\hat{q}^\dagger_{\nu_3}\hat{q}^\dagger_{\nu_2}\hat{q}_{\mu_2}\hat{q}_{\mu_3}. \tag{27}$$

The operator $\hat{\Delta}_{N'N}$ reflects the internal structure of nucleons, complicating the application of field-theoretic methods that rely on canonical (anti)commutation relations. Moreover, the two-nucleon state $|NN'\rangle = \hat{B}^\dagger_N\hat{B}^\dagger_{N'}|0\rangle$ would be normalized if nucleons were elementary particles. However, in this composite case, its norm is given by [19, 20, 22, 23]:

$$\langle NN'|NN'\rangle = 1 - \delta_{NN'} - K_{NN'}, \tag{28}$$

where

$$K_{NN'} = 3\Psi_N^{*\mu_1\mu_2\mu_3}\Psi_{N'}^{*\nu_1\nu_2\nu_3}\left(\Psi_N^{\mu_1\mu_2\nu_3}\Psi_{N'}^{\nu_1\nu_2\mu_3} - \Psi_N^{\mu_1\nu_2\nu_3}\Psi_{N'}^{\nu_1\mu_2\mu_3}\right). \tag{29}$$

This again highlights the inherent difficulties of working with composite field operators in many-body systems. Of course, the effects of the operator $\hat{\Delta}_{NN}$ become negligible when the nucleon density is low enough that their wavefunctions do not overlap. As in the case of composite bosons [24, 25], one can show that the effect of $\hat{\Delta}$ on the norm of a many-body state with N composite nucleons confined to a volume V scales as $(N/V) \times R_N^3$, where R_N characterizes the spatial extent of the nucleon wavefunction.

In what follows, I present preliminary results from an attempt to apply field-theoretical methods using nucleon field operators that effectively incorporate the internal structure of nucleons. Rather than employing complex many-quark composite operators, the approach relies on nucleon fields whose anticommutation relations deviate only minimally from the canonical fermionic form. Such operators were used by Greenberg in 1991 in the context of nonrelativistic field theory with the aim of setting experimental constraints on possible violations of the Pauli exclusion principle (Fermi statistics) and Bose statistics [26]. Applications of this framework to nonrelativistic bosons—to account for internal structure—can be found in Refs. [25, 27]. The literature on this subject is extensive; earlier results are referenced in these works, while a more recent relativistic generalization, relevant to the present study of nuclear matter, is provided in Ref. [28]. In this initial application, magnetic field effects are neglected. The focus is instead on equilibrium mean-field properties, which will serve as the starting point for future nonequilibrium studies, including magnetic field effects, as outlined in the previous section.

To make the discussion concrete, the results presented here are based on a Lagrangian density for nucleon fields ψ, Yukawa-coupled to isoscalar-scalar σ and isoscalar-vector ω_μ meson fields, the Walecka model [29]:

$$\mathcal{L} = \overline{\psi}\left[\gamma_\mu\left(i\partial^\mu - g_\omega\omega^\mu\right) - \left(m_N - g_\sigma\sigma\right)\right]\psi + \frac{1}{2}\left(\partial_\mu\sigma\partial^\mu - m_\sigma^2\sigma^2\right) - \frac{1}{4}F_{\mu\nu}F^{\mu\nu} + \frac{1}{2}\omega_\mu\omega^\mu, \tag{30}$$

where $F_{\mu\nu} = \partial_\mu\omega_\nu - \partial_\nu\omega_\mu$. In the mean-field approximation, the meson fields are treated as space- and time-independent classical fields, $\sigma(x) = \sigma_0$ and $\omega_\mu(x) = \omega_0\,\delta_{\mu 0}$. This choice of Lagrangian is made for simplicity; the approach can be extended to more sophisticated models. The composite nature of the nucleon quantum field $\hat{\psi}$ is incorporated through a noncanonical equal-time anticommutation relation [28]:

$$\hat{\psi}(\boldsymbol{x},t)\hat{\psi}^\dagger(\boldsymbol{x}',t) + \lambda\,\hat{\psi}^\dagger(\boldsymbol{x}',t)\hat{\psi}(\boldsymbol{x},t) = \delta(\boldsymbol{x}-\boldsymbol{x}') \quad \text{with} \quad 0 < \lambda \leq 1. \tag{31}$$

Introducing the deformation parameter ξ via $\lambda = 1 - \xi$, the relation becomes

$$\{\hat{\psi}(\boldsymbol{x},t), \hat{\psi}^\dagger(\boldsymbol{x}',t)\} = \delta(\boldsymbol{x}-\boldsymbol{x}') + \xi\,\hat{\psi}^\dagger(\boldsymbol{x}',t)\hat{\psi}(\boldsymbol{x},t). \tag{32}$$

Here, the operator term $\xi\,\hat{\psi}^\dagger(\boldsymbol{x}',t)\hat{\psi}(\boldsymbol{x},t)$ provides an effective representation of the operator $\hat{\Delta}$ defined in Eq. (27). Moreover, the parameter ξ is density-dependent: it vanishes at low densities and grows with increasing density. This interpretation of ξ as an effective measure of $\hat{\Delta}$'s contribution was substantiated in Refs. [25, 27] in the case of nonrelativistic composite bosons.

In this mean field approximation, the grand-canonical potential, function of temperature T and baryon chemical potential μ, is essentially the one of a free gas of noninteracting quasiparticles with an effective mass m_N^* and effective chemical potential μ^*:

$$m_N^* = m_N - \frac{g_\sigma^2}{m_\sigma^2}\,\rho_s(\lambda) \quad \text{and} \quad \mu^* = \mu + T\ln\lambda - \frac{g_\omega^2}{m_\omega^2}\,\rho(\lambda), \tag{33}$$

where the scalar and vector densities are given by (in the no-sea approximation):

$$\rho(\lambda) = \frac{1}{V}\int d^3x\, \langle \psi^\dagger(x)\psi(x)\rangle = \gamma \int \frac{d^3k}{(2\pi)^3}\left(\frac{1}{e^{\beta E(\boldsymbol{k})-\mu_\lambda}+\lambda} - \frac{1/\lambda}{\lambda\, e^{\beta E(\boldsymbol{k})+\mu_\lambda}+1}\right), \tag{34}$$

$$\rho_s(\lambda) = \frac{1}{V}\int d^3x\, \langle \bar\psi(x)\psi(x)\rangle = \gamma \int \frac{d^3k}{(2\pi)^3}\,\frac{m_N^*}{E(\boldsymbol{k})}\left(\frac{1}{e^{\beta E(\boldsymbol{k})-\mu_\lambda}+\lambda} + \frac{1/\lambda}{\lambda\, e^{\beta E(\boldsymbol{k})+\mu_\lambda}+1}\right), \tag{35}$$

with $E(\boldsymbol{k}) = (\boldsymbol{k}^2 + m_N^{*2})^{1/2}$ and $\gamma = 2$ for nuclear matter and $\gamma = 1$ for pure-neutron matter. The mean-field energy density is given by

$$\varepsilon = \frac{g_\omega^2}{2m_\omega^2}\rho_B^2(\lambda) + \frac{g_\sigma^2}{2m_\sigma^2}\rho_s^2(\lambda) + \gamma \int \frac{d^3k}{(2\pi)^3}\, E(\boldsymbol{k})\left(\frac{1}{e^{\beta E(\boldsymbol{k})-\mu_\lambda}+\lambda} + \frac{1/\lambda}{\lambda\, e^{\beta E(\boldsymbol{k})+\mu_\lambda}+1}\right). \tag{36}$$

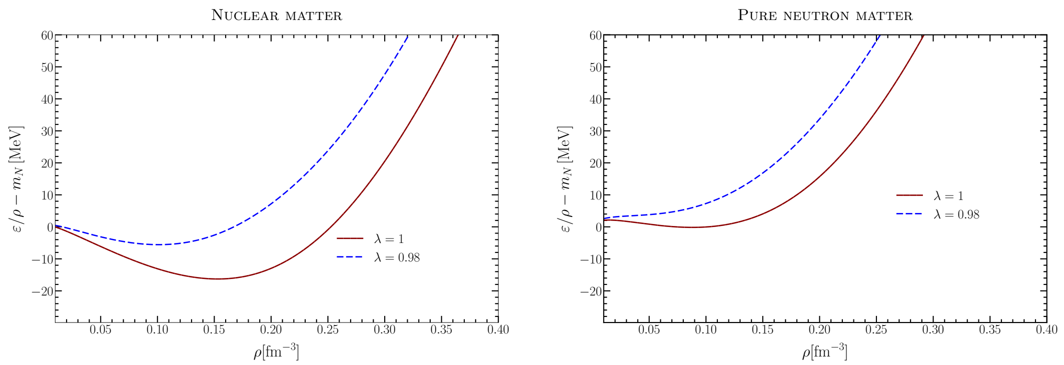

Figure 3: Binding energy per nucleon of nuclear matter and neutron matter.

To gain insight into the role of λ, Fig. 3 displays the zero-temperature binding energy, $\varepsilon/\rho - m_N$, assuming a density-independent λ. The figure shows that decreasing λ (i.e., increasing the deviation from canonical anticommutation relations) leads to enhanced repulsion in the binding energy. This behavior appears physically reasonable: as nucleons begin to overlap at high densities, the Pauli exclusion principle is expected to take effect at the quark level. Such effects have been observed in studies of low-energy hadron-hadron interactions within the quark model, where quark exchange combined with one-gluon exchange gives rise to short-range repulsion—see Refs. [21, 23] for a compilation of relevant studies.

Naturally, a more comprehensive understanding of the influence of the modified anticommutation relation in Eq. (32) requires making the deformation parameter ξ density-dependent. Its impact on other thermodynamic observables, such as the pressure, compressibility, and speed of sound, among others, also needs to be explored in future work.

4. Conclusions and Perspectives

I began by presenting selected results on the impact of strong magnetic fields on the time evolution of the chiral condensate in quark matter, obtained within the linear sigma model with quarks. The temporal dynamics of the condensate were described by a Ginzburg–Landau–Langevin (GLL) equation derived from a two-particle irreducible effective action, using the closed-time path formalism of nonequilibrium quantum field theory.

I then introduced a field-theoretical approach incorporating nucleon field operators with modified anticommutation relations to effectively account for quark substructure effects. Preliminary results, obtained in a model based on the Walecka Lagrangian treated in the mean-field approximation, show that these modifications introduce a repulsive contribution to the binding energy of both nuclear and pure neutron matter. This behavior is consistent with short-range repulsion arising from quark exchange in quark-model studies of hadron-hadron interactions.

The combination of these two frameworks—the closed-time path formalism for nonequilibrium dynamics and deformed nucleon operators to encode subnucleonic structure—offers a promising avenue for exploring one of the most challenging regions of the QCD phase diagram: low-temperature, moderate-density matter, where baryon densities range from one to about five times nuclear saturation. In this regime, nucleons begin to overlap spatially but have not yet dissolved into deconfined quarks and gluons, making it a testing ground for our understanding of strongly interacting matter.

Acknowledgments

I wish to thank Carlisson Miller and Arthur Frazon for the collaborative work on the dynamics of the chiral condensate. This work was partially financed by Fundação de Amparo à Pesquisa do Estado de São Paulo (FAPESP), grant no. 2018/25225-9, and Conselho Nacional de Desenvolvimento Científico e Tecnológico (CNPq), grant no. 309262/2019-4.

References

[1] P. Adhikari et al., *Strongly interacting matter in extreme magnetic fields*, 2412.18632.

[2] G. Endrodi, *QCD with background electromagnetic fields on the lattice: A review*, *Prog. Part. Nucl. Phys.* **141** (2025) 104153 [2406.19780].

[3] E.S. Fraga, L.F. Palhares and T.E. Restrepo, *Cold and dense perturbative QCD in a very strong magnetic background*, *Phys. Rev. D* **109** (2024) 054033 [2312.13952].

[4] G. Krein and C. Miller, *Nonequilibrium Dynamics of the Chiral Quark Condensate under a Strong Magnetic Field*, *Symmetry* **13** (2021) 551 [2103.15665].

[5] N. Goldenfeld, *Lectures on phase transitions and the renormalization group*, Perseus Books, Reading (1992).

[6] A. Onuki, *Phase Transition Dynamics*, Cambridge University Press, Cambridge (2002).

[7] M. Gell-Mann and M. Levy, *The axial vector current in beta decay*, *Nuovo Cim.* **16** (1960) 705.

[8] J.D. Bjorken and S.D. Drell, *Relativistic quantum fields*, .

[9] M. Nahrgang, S. Leupold, C. Herold and M. Bleicher, *Nonequilibrium chiral fluid dynamics including dissipation and noise*, *Phys. Rev. C* **84** (2011) 024912 [1105.0622].

[10] J.S. Schwinger, *Brownian motion of a quantum oscillator*, *J. Math. Phys.* **2** (1961) 407.

[11] L.V. Keldysh, *Diagram technique for nonequilibrium processes*, *Zh. Eksp. Teor. Fiz.* **47** (1964) 1515.

[12] R.P. Feynman and F.L. Vernon, Jr., *The Theory of a general quantum system interacting with a linear dissipative system*, *Annals Phys.* **24** (1963) 118.

[13] E.A. Calzetta and B.-L.B. Hu, *Nonequilibrium Quantum Field Theory*, Cambridge Monographs on Mathematical Physics, Cambridge University Press (9, 2008), 10.1017/CBO9780511535123.

[14] M.L. Bellac, *Thermal Field Theory*, Cambridge Monographs on Mathematical Physics, Cambridge University Press (3, 2011), 10.1017/CBO9780511721700.

[15] A. Frazon, *Thermalization Dynamics of the Quark Condensate Under Strong Magnetic Fields*, msc thesis, Instituto de Física Teórica, UNESP, 08, 2024.

[16] G. Baym, *Confinement of quarks in nuclear matter*, *Physica A* **96** (1979) 131.

[17] K. Fukushima, T. Kojo and W. Weise, *Hard-core deconfinement and soft-surface delocalization from nuclear to quark matter*, *Phys. Rev. D* **102** (2020) 096017 [2008.08436].

[18] A. Thomas, *Chiral symmetry and the bag model: A new starting point for nuclear physics*, *Adv. Nucl. Phys.* **13** (1984) 1.

[19] M. Betz, G. Krein and T.A.J. Maris, *BAGS IN THE SHELL MODEL*, *Nucl. Phys. A* **437** (1985) 509.

[20] G. Krein and T.A.J. Maris, *COMPATIBILITY OF THE NUCLEAR SHELL AND NUCLEON BAG MODELS*, *Phys. Rev. C* **36** (1987) 365.

[21] D. Hadjimichef, G. Krein, S. Szpigel and J.S. da Veiga, *Mapping of composite hadrons into elementary hadrons and effective hadronic Hamiltonians*, *Annals Phys.* **268** (1998) 105 [hep-ph/9805459].

[22] D. Blaschke and G. Ropke, *PAULI QUENCHING FOR HADRONS IN NUCLEAR MATTER: A QUARK SUBSTRUCTURE EFFECT*, .

[23] D. Blaschke, H. Grigorian and G. Röpke, *Chirally improved quark Pauli blocking in nuclear matter and applications to quark deconfinement in neutron stars*, *Particles* **3** (2020) 477 [2005.10218].

[24] H.J. Lipkin, *Quantum Mechanics: New Approaches to Selected Topics*, North-Holland Pu. Co. (1989).

[25] S.S. Avancini and G. Krein, *Many body problems with composite particles and q Heisenberg algebras*, *J. Phys. A* **28** (1995) 685.

[26] O.W. Greenberg, *Particles with small violations of fermi or bose statistics*, *Phys. Rev. D* **43** (1991) 4111.

[27] S.S. Avancini, J.R. Marinelli and G. Krein, *Compositeness effects in the Bose-Einstein condensation*, *J. Phys. A* **36** (2003) 9045 [cond-mat/0210310].

[28] X.-Y. Hou, H. Yan and H. Guo, *Thermostatistics of a q-deformed Relativistic Ideal Fermi Gas*, *J. Stat. Mech.* **2011** (2020) 113402 [2006.04392].

[29] J.D. Walecka, *A Theory of highly condensed matter*, *Annals Phys.* **83** (1974) 491.